ANNUAL AND MONTHLY MEAN GLOBAL, DIRECT AND DIFFUSE SOLAR IRRADIATION IN BOTUCATU/SP/BRAZIL

[1] João F. Escobedo; [1] Douglas Rodrigues; [2] Amauri P. Oliveira; [2] Jacyra Soares

1 – Department of Natural Resources/Environmental Sciences – FCA/UNESP/Botucatu/SP/Brazil

2 – Department of Atmospheric Sciences – IAG/USP/São Paulo/SP/Brazil

Abstract: This paper presents a climatic and statistical analysis of global, direct horizontal and diffuse radiation from a database of solar radiation measured from 1996 to 2006 in the city of Botucatu, SP, Brazil. Variation intervals of hourly and daily irradiation, annual mean $<\bar{H}_G>$, $<\bar{H}_{bh}>$ and $<\bar{H}_d>$ irradiation, monthly mean $<\bar{H}_G>$, $<\bar{H}_{bh}>$ and $<\bar{H}_d>$ irradiation and monthly mean $<\bar{K}t>$, $<\bar{K}_{bh}>$ and $<\bar{K}_d>$ fractions were determined. Results showed that values of hourly and daily annual mean irradiation were as follows: $<\bar{H}_G>=1.49$MJ/m^2 and $<\bar{H}_G>=17.74$MJ/m^2; $<\bar{H}_{bh}>=0.90$MJ/m^2 and $<\bar{H}_{bh}>=10.33$MJ/m^2 and $<\bar{H}_d>=0.57$ MJ/m^2 and $<\bar{H}_d>=7.09$MJ/m^2, respectively. Variation intervals of hourly monthly mean irradiation were as follows: $<\bar{H}_G>$ ranged from 1.65MJ/m^2 in March to 1.16MJ/m^2 in June; $<\bar{H}_{bh}>$ ranged from 1.06MJ/m^2 in April to 0.79MJ/m^2 in June, and $<\bar{H}_d>$ ranged from 0.70MJ/m^2 in January to 0.37MJ/m^2 in June and July. Similarly, daily $<\bar{H}_G>$ irradiation ranged from 21.35MJ/m^2 in November to 12.94MJ/m^2 in June; $<\bar{H}_{bh}>$ ranged from 11.83MJ/m^2 in April to 8.49MJ/m^2 in June, and $<\bar{H}_d>$ ranged from 10.29MJ/m^2 in December to 4.38MJ/m^2 in June. Variation intervals of hourly monthly mean fractions were as follows: $<\bar{K}t>$ ranged from 43.5% in January to 54.2% in April; $<\bar{K}_{bh}>$ ranged from 33.6% in January to 58.0% in April and $<\bar{K}_d>$ ranged from 66.4% in January to 42.0% in April. In the same way, daily $<\bar{K}t>$ fractions ranged from 45.5% in January to 59.8% in August; $<\bar{K}_{bh}>$ ranged from 38.9% in January to 62.0% in August and $<\bar{K}_d>$ ranged from 61.1% in January to 37.7% in July.

1. INTRODUCTION

Knowledge of global (G), direct horizontal (b_h) and diffuse (d) solar radiation by means of temporal and spatial series or estimation models is of major importance for developing research or simulation projects in areas of Engineering, Forestry and Agricultural Sciences. Studies in the literature have shown that most of them have been conducted using estimation models, which associate the clarity index Kt ($Kt=G/H_0$, where H_0 is the extraterrestrial radiation) with K_{bh} (b_h/G) direct fraction and K_d (d/G) diffuse fraction of global radiation, as shown in studies developed by De Miguel *et al.* (2001); Erbs (1982); Reindl (1990); Hawlader (1984); Oliveira (2002b); Louche *et al.* (1991); Lam and Li (1996); Lalas *et al.* (1987); Newland (1989); Jacovides *et al.* (1996); Soares, *et al.* (2004) and others. Studies on the series of G, b_h and d radiation are a result of measurements in time and space. In Brazil, a country of continental dimension with regions having different climate conditions, simultaneous measurements of two of these components in only one site are still scarce, and little information is available in the literature as shown in studies by Sousa *et al.* (2005); Tiba *et al.* (2005); Oliveira *et al*. (2002a); Cavalcanti (1991). The major limitation of few measurement sites of direct at normal incidence, or diffuse radiation is the high cost of pyreliometers on a solar tracker and pyranometers equipped with shadow rings used to measure diffuse radiation. These devices have still been imported at high cost. For information on the three types of radiation in a single site, the Solar Radiometric Station monitored G radiation and b_h radiation at normal incidence in the period of 1996 to 2006 in Botucatu/SP/Brazil. The research will contribute to studies on conversion processes of thermal, photovoltaic and biomass energy, as well as on climatology and environmental studies. Several microclimatic meteorological events have happened annually in the local atmosphere, which increased considerably cloudiness and precipitation in the summer and spring (rainy period), while high concentrations of aerosol as a result of sugar cane burning were observed in autumn and winter (dry period). The effects of sky coverage and climatic changes on values of the three types of radiation have remained unknown in the site of the study. Therefore, this initial study shows a statistical analysis of annual and monthly mean global,

direct and diffuse irradiation among years. Results were analyzed and discussed as a function of climatic changes occurred in the same period of measurement.

2. METHODOLOGY

2.1. Climate description

Measurements were performed in the Solar Radiometric Station in Botucatu city, School of Agricultural Sciences, State University of São Paulo (22º53'S latitude, 48º26'W longitude and 786 m altitude). A warm temperate mesothermal climate is dominant in the area and characterized by precipitation in the summer and drought in the winter. Figure 1(a, b, c) shows climatic series of temperature, relative humidity, cloudiness and precipitation from 1970 to 2000 in Botucatu city. Temperature and humidity are higher when solar declination is closer to the local latitude, and lower when the sun declines in the northern hemisphere, farther to the local latitude. February and July are the hottest (23.2ºC mean temperature) and the coldest (17.1ºC mean temperature) months, respectively. February is the most humid month and August is the driest month with relative humidity of 78.2% and 61.80%, respectively.

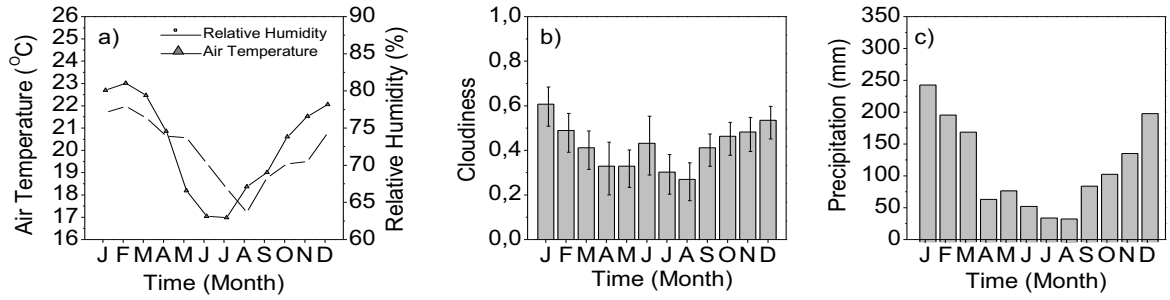

Fig. 1(a, b, c): Climatic series of temperature (a), humidity (a), cloudiness (b) and precipitation (c) from 1970 to 2000 in Botucatu.

In most months, annual evolution of cloudiness (Fig. 1b) follows the values of temperature and relative humidity of the climatic series. The highest and lowest values of cloudiness are found in January (f=0.61) and August (f=0.27), respectively. Conversely, the highest number of sunshine hours is in August and the lowest one is in February with a total of 229 hours and 175.28 hours, respectively. The longest day in December (summer solstice) has 13.4 hours and the shortest day in June (winter solstice) has 10.6 hours. Annual evolution of monthly mean precipitation follows the evolution of cloudiness (Fig. 1c). It consists of two distinct rainy and dry periods, in which the limit between the periods is the precipitation value of 100 mm, approximately. The highest values of precipitation occur in January and reach 260.7 mm, whereas the lowest values occur in August and reach 38.2 mm.

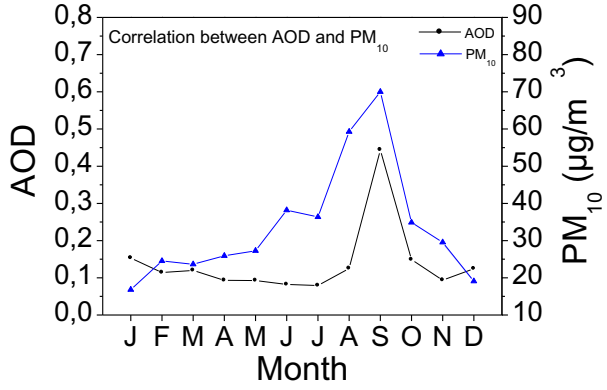

Fig. 2: Monthly correlation between aerosol optical depth (AOD) and concentration of particulate matter, PM_{10} in $\mu g.m^{-3}$ in 2004, Botucatu.

The city of Botucatu has 100 thousand inhabitants and does not have large polluting industries. However, it is located in a rural area of sugar cane crops and ethanol production. During the dry period and at the beginning of the rainy period (July to November), the local atmosphere shows high concentration values of particulates originated from burning of sugarcane debris and industries of ethanol and sugar production located within 100 km from the city center. Annual evolution of mean AOD obtained by the TERRA satellite in 2004 (Fig. 2) shows that from the beginning of sugarcane burning in July, the monthly concentration values of aerosol increase considerably reaching a maximum value of AOD=0.45 in September. This value is equivalent to PM_{10} concentration of 70.0 $\mu g.m^{-3}$ (Codato *et al.*, 2008).

2.2. Instrumentation

Global irradiance (I_G) was monitored by an Eppley PSP pyranometer. Direct irradiance at normal incidence (I_b) was monitored by an Eppley NIP pyreliometer mounted on an Eppley ST-3 solar tracker. Diffuse irradiation (I_d) was obtained by the difference between I_G irradiance and direct irradiance on the horizontal surface (I_{bh}), calculated at the same frequency, using the equation $I_d = I_G - I_{bh} = I_G - I_b \cos z$, in which z is the zenith angle.

Measurement errors of global and direct radiation are related to the precision of the Eppley equipment: the PSP pyranometer, which measures global radiation, has an uncertainty of approximately 1.5% to 2.0%, and the pyreliometer, which measures direct radiation, has an uncertainty of 1.5% to 2.0%. Therefore, the diffuse radiation has an estimated error of 3.5% to 4.0%.

For data acquisition, a Campbell Scientific CR23X data logger with a sampling frequency of 1 Hz was used. They were collected every 1 second interval and 5-min means were stored. The data underwent quality control and spurious values were removed. Then, integration of hourly, daily and monthly radiation values was performed using computer programs.

3. Results

3.1. Annual mean $\bar{H}_G$, $\bar{H}_{bh}$ and $\bar{H}_d$ irradiation

The statistical analysis of annual mean irradiation in Tab. 1 shows the number of hours and days of irradiation, mean values of global, direct and diffuse irradiation per year with percent standard deviations. The $\bar{H}_G$, $\bar{H}_{bh}$ and $\bar{H}_d$ lines (hourly and daily) show values of annual mean irradiation calculated for each year in MJ/m^2 in the period from 1996 to 2006 using the Eq. 1, in which $\delta\bar{H}_G$, $\delta\bar{H}_{bh}$ and $\delta\bar{H}_d$ are percent standard deviations of annual mean irradiation. The $<\bar{H}_G>$, $<\bar{H}_{bh}>$ and $<\bar{H}_d>$ lines show values among years of annual mean irradiation in MJ/m^2 calculated using the Eq. 2, in which $\delta<\bar{H}_G>$, $\delta<\bar{H}_{bh}>$ and $\delta<\bar{H}_d>$ are percent standard deviations of annual mean irradiation among years.

$$\bar{\mathbf{H}}_{\mathbf{G}} = \sum_{\mathbf{i=1}}^{\mathbf{n}}(\mathbf{H_G}/\mathrm{n});\ \bar{\mathbf{H}}_{\mathbf{bh}} = \sum_{\mathbf{i=1}}^{\mathbf{n}}(\bar{\mathbf{H}}_{\mathbf{bh}}/\mathrm{n});\ \bar{\mathbf{H}}_{\mathbf{d}} = \sum_{\mathbf{i=1}}^{\mathbf{n}}(\bar{\mathbf{H}}_{\mathbf{d}}/\mathrm{n}) \quad (1)$$

$$<\bar{\mathbf{H}}_{\mathbf{G}}> = \sum_{\mathbf{j=1}}^{\mathbf{m}}(\bar{\mathbf{H}}_{\mathbf{G}}/\mathbf{m});\ <\bar{\mathbf{H}}_{\mathbf{bh}}> = \sum_{\mathbf{j=1}}^{\mathbf{m}}(\bar{\mathbf{H}}_{\mathbf{bh}}/\mathbf{m});\ <\bar{\mathbf{H}}_{\mathbf{d}}> = \sum_{\mathbf{j=1}}^{\mathbf{m}}(\bar{\mathbf{H}}_{\mathbf{d}}/\mathbf{m}) \quad (2)$$

in which, n is the number of hours and days and j is the number of years.

Fig. 3 shows values of daily $<\bar{H}_G>$, $<\bar{H}_{bh}>$ and $<\bar{H}_d>$ irradiation with standard deviations. The line with bars represents mean values of global, direct and diffuse irradiation among years, with standard deviations. Mean values of global, direct and diffuse irradiation among years were as follows:

hourly $<\bar{H}_G>=(1.49\pm0.07 MJ/m^2)$ and daily $<\bar{H}_G>=(17.74\pm0.48 MJ/m^2)$;

hourly $<\bar{H}_{bh}>=(0.9\pm0.07 MJ/m^2)$ and daily $<\bar{H}_{bh}>=(10.33\pm0.57\ MJ/m^2)$;

hourly $<\bar{H}_d>=(0.57\pm0.04 MJ/m^2)$ and daily $<\bar{H}_d>=(7.09\pm0.4 MJ/m^2)$.

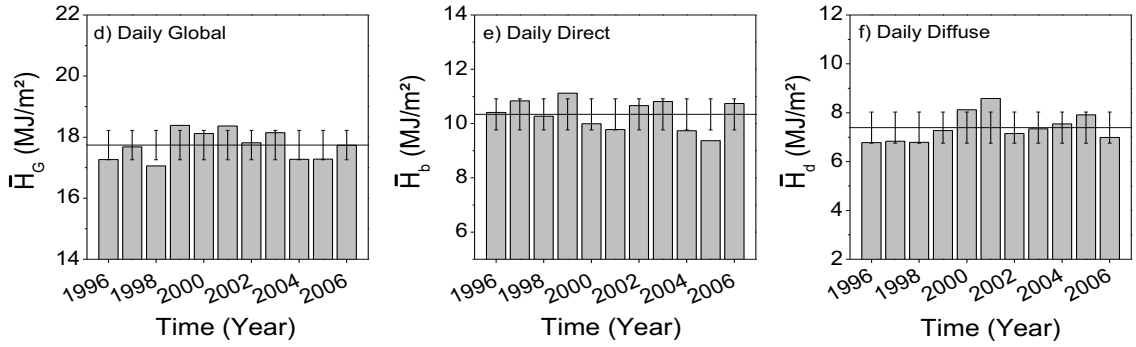

Fig.3: Mean irradiation inter years and annual mean global, direct and diffuse irradiation from 1996 to 2006.

Tab. 1: Number of hours and days, annual mean with standard deviations for global, direct and diffuse irradiation per year

Year	Radiation	Nº of Hours	Annual Mean (MJ/m²)	Deviation (%)		Nº of Days	Annual Mean (MJ/m²)	Deviation (%)
1996	$\bar{H}_G$	3131	1.50	67.9		262	17.26	31.4
	$\bar{H}_{bh}$	3131	0.91	99.5		262	10.41	60.4
	$\bar{H}_d$	3131	0.59	82.3		262	6.78	50.2
1997	$\bar{H}_G$	4019	1.54	68.2		342	17.68	34.7
	$\bar{H}_{bh}$	4019	0.95	99.2		342	10.84	63.3
	$\bar{H}_d$	4019	0.59	83.5		342	6.83	51.7
1998	$\bar{H}_G$	3919	1.52	68.1		349	17.06	37.7
	$\bar{H}_{bh}$	3919	0.92	98.9		349	10.27	66.8
	$\bar{H}_d$	3919	0.60	75.4		349	6.79	41.9
1999	$\bar{H}_G$	4081	1.53	72.5		334	18.39	33.7
	$\bar{H}_{bh}$	4081	0.94	100.3		334	11.12	60.8
	$\bar{H}_d$	4081	0.60	78.8		334	7.27	41.7
2000	$\bar{H}_G$	4336	1.45	75.9		364	18.12	34.1
	$\bar{H}_{bh}$	4336	0.84	108.5		364	9.99	64.8
	$\bar{H}_d$	4336	0.61	83.3		364	7.77	43.9
2001	$\bar{H}_G$	4068	1.49	73.6		348	18.37	33.8
	$\bar{H}_{bh}$	4068	0.86	107.3		348	9.78	69.3
	$\bar{H}_d$	4068	0.63	85.5		348	7.92	45.8
2002	$\bar{H}_G$	4129	1.46	73.5		348	17.81	32.7
	$\bar{H}_{bh}$	4129	0.90	103.7		348	10.67	61.6
	$\bar{H}_d$	4129	0.55	89.3		348	6.80	53.1
2003	$\bar{H}_G$	3817	1.55	69.3		352	18.15	33.3
	$\bar{H}_{bh}$	3817	1.00	97.0		352	10.81	66.0
	$\bar{H}_d$	3817	0.55	91.1		352	6.83	57.9
2004	$\bar{H}_G$	4121	1.41	74.8		358	17.28	37.3
	$\bar{H}_{bh}$	4121	0.85	109.8		358	9.74	73.0
	$\bar{H}_d$	4121	0.56	86.4		358	7.03	51.1
2005	$\bar{H}_G$	4095	1.40	73.5		357	17.28	34.4
	$\bar{H}_{bh}$	4095	0.82	112.7		357	9.31	74.0
	$\bar{H}_d$	4095	0.58	88.6		357	7.16	51.6
2006	$\bar{H}_G$	3131	1.50	67.9		364	17.73	30.4
	$\bar{H}_{bh}$	3131	0.91	99.5		364	10.74	60.9
	$\bar{H}_d$	3131	0.59	82.3		364	6.99	53.9
Inter-annual	$\langle\bar{H}_G\rangle$	11	1.49	3.4		11	17.74	2.7
	$\langle\bar{H}_{bh}\rangle$	11	0.90	6.0		11	10.33	5.5
	$\langle\bar{H}_d\rangle$	11	0.57	4.3		11	7.09	5.6

The percent deviation D_V (%) between annual mean irradiation and inter years mean irradiation from 1996 to 2006, calculated by the Eq. 3, expresses the variability of irradiation in each year. The result is shown in Fig. 4.

$$D_V = \left(\frac{\text{Annual Mean Irradiation} - \text{inter years Mean Irradiation}}{\text{inter years Mean Irradiation}}\right) * 100 \qquad (3)$$

The percent deviations were different among years for the 3 types of radiation. For hourly global irradiation, the deviations (D_V%) ranged from -5.4% to 4.8%, whereas for daily global irradiation they ranged from -3.8% to 3.6%. For hourly direct irradiation, the deviations (D_V%) ranged from -6.2% to 11.6%, whereas for daily direct irradiation, they ranged from -9.4% to 7.6%. For hourly diffuse irradiation, the deviations (D_V%) ranged from -5.8% to 8.0%, whereas for daily diffuse irradiation, they ranged from -8.3% to 16.2%.

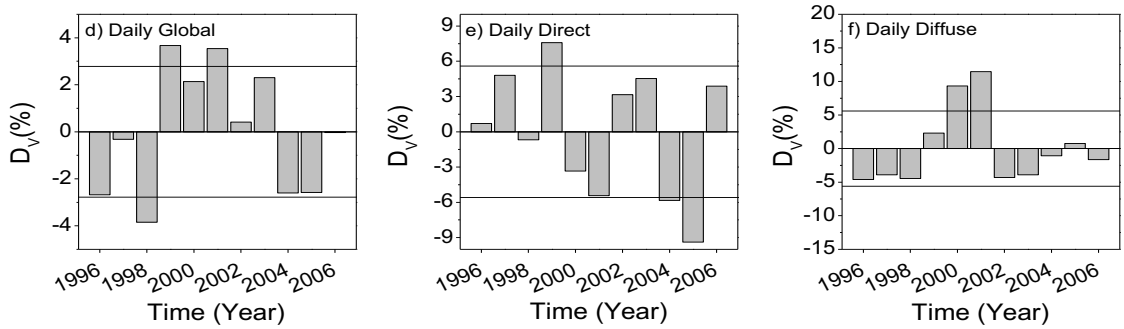

Fig.4: Percent deviation between annual mean irradiation and inter years annual mean irradiation from 1996 to 2006.

The annual mean value of irradiation, below or above the inter years mean value ± standard deviation, is not in agreement with that estimated by the 11-year series. Fig. 3 shows that mean values of global, direct and diffuse irradiation, in most years, are in agreement with those estimated by the experimental series from 1996 to 2006. The exceptions for hourly global radiation occurred in the years of 2003, 2004 and 2005, in which the standard deviations were higher than ±3.8% standard deviation of the total series. Daily global radiation exceptions occurred in the years of 1998, 1999 and 2001, in which the standard deviations were higher than ±2.8% standard deviation of the total series. Similarly, exceptions for hourly direct radiation were in 2003 and 2005, in which the standard deviations were higher than ±6.4% standard deviation of the total series. Exceptions for daily direct radiation occurred in 1999 and 2005 and the standard deviations were higher than ±5.6% standard deviation of the total series. Exceptions for hourly diffuse radiation occurred in 2001, 2002, 2003 and 2006, in which the standard deviations were higher than ±4.8% standard deviation of the total series. The exceptions for daily diffuse radiation occurred in 2000 and 2001, in which the standard deviations were higher than ±5.6% standard deviation of the total series.

The variability of global, direct and diffuse irradiation among years is highly associated with annual mean cloudiness and presence of water vapor in the atmosphere during the same period, which is caused mainly by synoptic systems: 1) Frontal systems (South Pole and Atlantic Ocean) as a result of polar cold fronts or humid fronts which cause an increase in cloudiness and precipitation of moderate and high intensity, mainly during austral autumn, winter and spring (Satyamurty & Mattos, 1989; Satyamurty *et al.*, 1998). According to Lemos & Calbete (1996), 5 events of frontal systems occur each month in the state of São Paulo. 2) The Convergence Zone of the South Atlantic Ocean (CZSA) characterized as a northwest-southeast oriented band of cloudiness from the Amazon Basin to the South Atlantic Ocean, is a result of the convergence of hot and humid air masses from the Amazon Basin and the South Atlantic Ocean. The CZSA causes an increase in cloudiness and intense and persistent precipitation events between the end of the austral spring and the beginning of autumn Liebmann *et al.*, 2001; Carvalho *et al.*, 2002. The frequency of occurrence is twice to four times a year, mean duration of 8 days and variable intensity (Nogués-Paegle & Mo, 1997).

The annual mean global irradiation in 1998 was lower than the mean value of the series with no significant increase in cloudiness, water vapor and accumulated precipitation in that year. On the contrary, both meteorological parameters remained within the interval estimated by the climatic series (Fig. 5a, c).

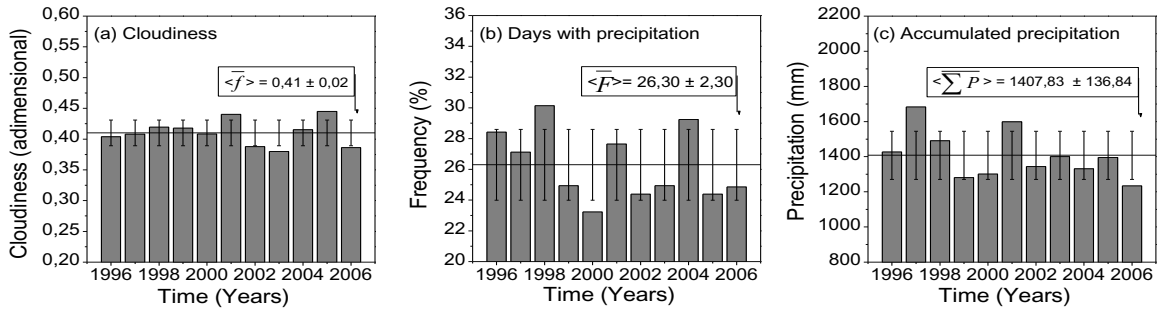

Fig. 5: a) Daily annual mean cloudiness; b) Days with precipitation; c) Annual accumulated precipitation, from 1996 to 2006.

However, Figure 5b shows that during that year, an unusual increase in the frequency of rainy days, in relation to the mean value, occurred as a result of CZSA and frontal systems. CZSA and frontal systems which occurred that year caused an increase in cloudiness; and the precipitation was of low intensity with long duration in both seasons (summer and spring), in which the value of radiation energy in the year is higher. The increased cloudiness in that year led to an increased diffuse radiation. The increased water vapor concentration led to an increased absorption of infrared radiation and therefore to a decreased global radiation. In this study, only days with accumulated precipitation higher than 1mm were considered as days of precipitation. The unusual increase in global radiation in 2001 occurred as a consequence of cold front passages from the South Pole, which increased, in an unusual way, cloudiness, precipitation and water vapor in the dry season, during autumn and winter. The phenomenon caused a decrease in direct radiation and an increase in the diffuse component in the seasons which have high direct and low diffuse radiation distribution. Annual mean direct irradiation in 1999 was high as a result of decreased cloudiness and precipitation, whereas low annual mean direct irradiation in 2005 was a consequence of an atypical increase in cloudiness and precipitation.

3.2. Annual evolution of monthly mean $\bar{H}_G$, $\bar{H}_{bh}$ and $\bar{H}_d$ irradiation

Table 1 shows annual evolution of monthly mean global, direct and diffuse (hourly and daily) irradiation from 1996 to 2006. The $<\bar{H}_G>$, $<\bar{H}_{bh}>$ and $<\bar{H}_d>$ columns show values among years of monthly mean irradiation in MJ/m^2 calculated using the Eq. 5, in which $\delta<\bar{H}_G>$, $\delta<\bar{H}_{bh}>$ and $\delta<\bar{H}_d>$ columns represent percent standard deviations. The $\bar{H}_G$, $\bar{H}_{bh}$ and $\bar{H}_d$ values (hourly and daily) of monthly mean irradiation were calculated for each year in MJ/m^2 using the Eq. 4.

$$\bar{\boldsymbol{H}}_{\boldsymbol{G}} = \sum_{i=1}^{n}(\boldsymbol{H}_{\boldsymbol{G}}/n);\ \bar{\boldsymbol{H}}_{\boldsymbol{bh}} = \sum_{i=1}^{n}(\boldsymbol{H}_{\boldsymbol{bh}}/n);\ \bar{\boldsymbol{H}}_{\boldsymbol{d}} = \sum_{i=1}^{n}(\boldsymbol{H}_{\boldsymbol{d}}/n) \quad (4)$$

$$< \bar{\boldsymbol{H}}_{\boldsymbol{G}} > = \sum_{j=1}^{m}(\bar{\boldsymbol{H}}_{\boldsymbol{G}}/\boldsymbol{m});\ < \bar{\boldsymbol{H}}_{\boldsymbol{bh}} > = \sum_{j=1}^{m}(\bar{\boldsymbol{H}}_{\boldsymbol{bh}}/\boldsymbol{m});\ < \bar{\boldsymbol{H}}_{\boldsymbol{d}} > = \sum_{j=1}^{m}(\bar{\boldsymbol{H}}_{\boldsymbol{d}}/\boldsymbol{m}) \quad (5)$$

in which, n is the number of hours and days per year and j is the number of years.

Seasonality of $<\bar{H}_G>$, $<\bar{H}_{bh}>$ and $<\bar{H}_d>$ irradiation (hourly and daily) shown in Fig. 6 (a and b) is a result of astronomical and geographic changes, such as solar declination and latitude, and also of local climatic changes, such as clouds, water vapor and aerosols. Values of $<\bar{H}_G>$ and $<\bar{H}_d>$ irradiation were higher in the rainy period, negative solar declination and closer to the local latitude during January, February, March, October, November and December. In these months (Fig. 7), higher concentrations of water vapor and clouds in the atmosphere are observed. Conversely, values of irradiation were lower in the dry period, north solar declination and farther from local latitude during April, May, June, July, August and September. In these months, cloud and water vapor concentrations are the lowest, and aerosol concentration is the highest in the year (Fig. 7).

Seasonality of $<\bar{H}_{bh}>$ irradiation did not follow the same pattern of $<\bar{H}_G>$ and $<\bar{H}_d>$ irradiation. The value of $<\bar{H}_{bh}>$ was increasingly higher in April, March, August and September, with alternating cloudy and humid conditions in March and September and clearer and drier ones in April and August.

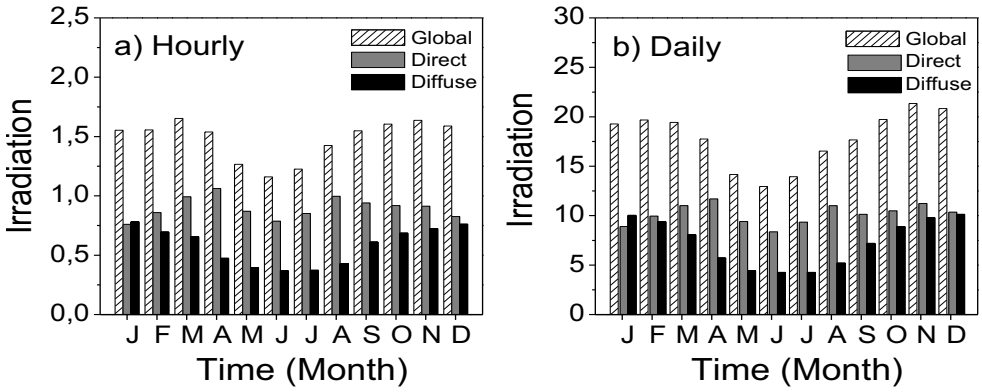

Fig. 6(a, b) shows annual evolution of hourly and daily, monthly mean $\bar{H}_G$, $\bar{H}_{bh}$ and $\bar{H}_d$ radiation among years.

Tab. 2: Values of $<\bar{H}_G>$, $<\bar{H}_{bh}>$ and $<\bar{H}_d>$ irradiation in MJ/m^2 from 1996 to 2006 and standard deviations in percentage.

Irradiation (MJ/m²) – Inter-Year mean												
	Hourly						**Daily**					
	Global		**Direct**		**Diffuse**		**Global**		**Direct**		**Diffuse**	
	$<\bar{H}_G>$	$\delta<\bar{H}_G>$	$<\bar{H}_{bh}>$	$\delta<\bar{H}_{bh}>$	$<\bar{H}_d>$	$\delta<\bar{H}_d>$	$<\bar{H}_G>$	$\delta<\bar{H}_G>$	$\bar{H}_{bh}$	$\delta<\bar{H}_{bh}>$	$<\bar{H}_d>$	$\delta<\bar{H}_d>$
Jan	1.55	11.6	0.77	22.1	0.79	10.1	19.26	10.4	9.05	21.6	10.21	7.5
Feb	1.56	12.8	0.85	28.3	0.70	8.6	19.52	10.9	10.03	24.1	9.50	9.7
Mar	1.65	7.9	0.99	18.2	0.66	15.2	19.49	7.0	11.29	21.8	8.20	15.8
Apr	1.54	7.1	1.06	13.2	0.48	14.6	17.73	7.7	11.83	15.3	5.89	12.6
May	1.27	6.3	0.87	13.8	0.40	15.0	14.18	7.3	9.57	15.1	4.61	15.4
Jun	1.16	5.2	0.79	13.9	0.37	18.9	12.94	8.4	8.49	17.0	4.38	19.2
Jul	1.23	4.9	0.85	8.2	0.37	10.8	13.95	4.2	9.52	8.7	4.43	11.3
Aug	1.42	6.3	0.99	15.2	0.43	18.6	16.53	7.7	11.17	17.1	5.36	19.2
Sept	1.55	4.5	0.94	10.6	0.61	9.8	17.66	7.6	10.29	13.6	7.37	8.6
Oct	1.60	8.1	0.92	16.3	0.69	10.2	19.74	9.7	10.65	16.6	9.08	12.3
Nov	1.64	7.3	0.91	17.6	0.72	9.7	21.35	5.2	11.37	17.3	9.97	13.4
Dec	1.59	6.9	0.83	15.7	0.76	6.6	20.79	6.3	10.50	15.4	10.3	9.3

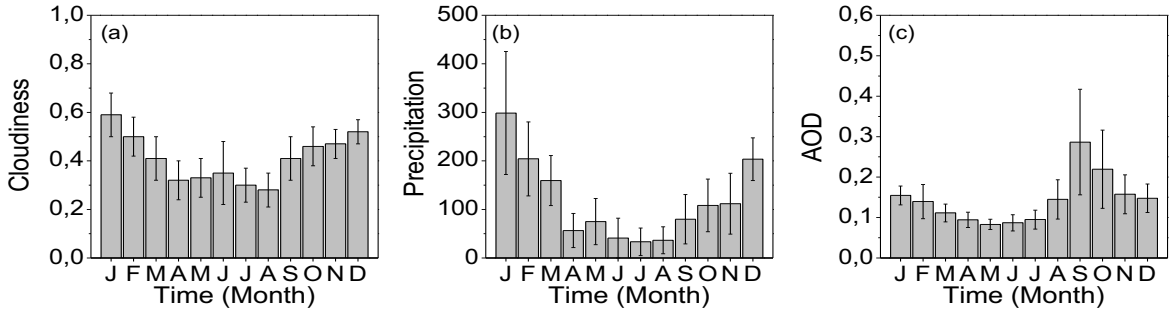

Fig 7: Monthly mean values of cloudiness (a), accumulated precipitation (b) in the experimental period (1996 to 2006), and. monthly mean values of AOD (c) obtained by the TERRA satellite from 2000 to 2005.

In general, $<\bar{H}_{bh}>$ value was lower in cloudy and humid months as January, February, June and December, except for June which is a dry and clear month. Hourly $<\bar{H}_G>$ irradiation ranged from 1.65MJ/m^2 (March) to 1.16MJ/m^2 (June), $<\bar{H}_{bh}>$ irradiation ranged from 1.06MJ/m^2 (April) to 0.79MJ/m^2 (June), and $<\bar{H}_d>$ irradiation

ranged from 0.70MJ/m^2 (January) to 0.37MJ/m^2 (June and July). Similarly, daily $<\bar{H}_G>$ irradiation ranged from 21.35MJ/m^2 (November) to 12.94MJ/m^2 (June), $<\bar{H}_{bh}>$ irradiation ranged from 11.83MJ/m^2 (April) to 8.49MJ/m^2 (June), and $<\bar{H}_d>$ irradiation ranged from 10.29MJ/m^2 (December) to 4.38MJ/m^2 (June).

The $\delta<\bar{H}_G>$, $\delta<\bar{H}_{bh}>$ and $\delta<\bar{H}_d>$ standard deviations shown in Figure 8 express the variability of hourly and daily $<\bar{H}_G>$, $<\bar{H}_{bh}>$and $<\bar{H}_d>$ irradiation in each month among years, and they were increasingly higher according to the sequence $\bar{H}_{bh}$, $\bar{H}_d$ and $\bar{H}_G$ irradiation. The variation range of irradiation is associated with the occurrence of CZSA macroclimatic events and the Humid Frontal System among years, which caused marked changes in cloudiness, precipitation and water vapor concentrations in the atmosphere in the rainy period (January, February, March, October, November and December). The occurrence of macroclimatic events in the dry period was a result of the Polar Frontal System among years, which caused marked changes in cloudiness and precipitation in May, June and July, and also, of burning of sugar cane among years which increased concentration of particulate matter in the atmosphere (August and September).

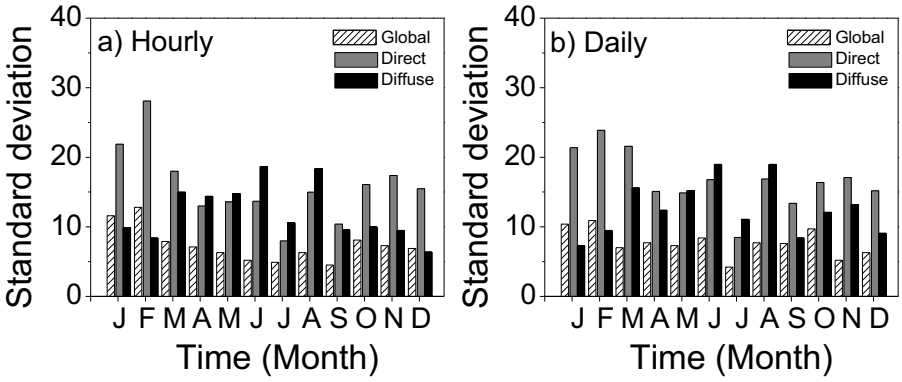

Fig. 8: Annual evolution of hourly and daily monthly mean $\delta<\bar{H}_G>$, $\delta<\bar{H}_{bh}>$ and $\delta<\bar{H}_d>$ standard deviations among years.

Values of $\delta<\bar{H}_{bh}>$ were higher in January, February and March, in which occurrence of CZSA was observed in at least one of the months, in the years of 1996, 1997, 1999, 2001, 2003, 2004 and 2005. Similarly, values of $\delta<\bar{H}_{bh}>$ were higher in October, November and December. Occurrence of the Humid Frontal System was observed in 1996, 1997, 1998, 2003 and 2005. Values of $\delta<\bar{H}_{bh}>$ were lower during the dry period of July and September. In the months of April, May, June and August, values of $\delta<\bar{H}_{bh}>$ were higher because of the occurrence of the Polar Frontal System in at least one of the months in the years of 1997, 1998, 1999, 2002, 2003,2004 and 2005. Also, variation in particulate matter concentrations in the atmosphere was also observed in August, from 2000 to 2006.Values of $\delta<\bar{H}_d>$ were higher in April, May, July and August, the dry period, as a consequence of occurrence of the Polar Frontal System, in at least one of the months in 1997, 1998, 1999, 2002, 2003, 2004 and 2005. Also, variation in concentration of particulate matter in the atmosphere was observed in August from 2000 to 2006. Values of $\delta<\bar{H}_d>$ were higher in March, October and November, the rainy period, because of occurrence of CZSA in at least one of the months in 1996, 2003 and 2006 and of the Humid Frontal System in 1997, 1998, 2000, 2003 and 2005. Hourly standard deviation ranged as it follows: $\delta<\bar{H}_G>$ from 11.6% in January to 4.5% in September; $\delta<\bar{H}_{bh}>$ from 28.3% in February to 8.2% in July and $\delta<\bar{H}_d>$ from 18.9% in June to 8.6% in February. Similarly, daily standard deviation ranged as follows: $\delta<\bar{H}_G>$ from 10.9% in February to 4.2% in July; $\delta<\bar{H}_{bh}>$ from 28.3% in February to 8.7% in July and $\delta<\bar{H}_d>$ from 19.2% in June to 7.5% in February.

3.4 Annual evolution of monthly mean $<\bar{K}t>$, $<\bar{K}_{bh}>$ and $<\bar{K}_d>$ fractions inter years.

Normalization of H_G irradiation by means of irradiation at the top of the atmosphere (H_0) defines the clearness index $Kt=H_G/H_0$, or atmospheric transmissivity of global irradiation, which eliminates the dependence of H_G irradiation from solar declination and local latitude. Therefore, Kt value is the general indicator of scattering and

absorption processes by clouds, water vapor and aerosols which reduce global radiation, and consequently, direct and diffuse irradiation in each month of the year. Fig. 9(a, b) shows values of $<\bar{K}t>$ fractions among years, calculated by Eq. 6.

$$< \bar{K}_t > = \sum_{j=1}^{m} (\bar{K}_t / m) \qquad (6)$$

in which, $\bar{K}_t = \sum_{i=1}^{n} (H_G / H_{0_i})/\mathrm{n}$

and n is the number of hours and days per year, and j is the number of years.

The comparison between annual evolution of daily $<\bar{K}t>$ (Fig. 9b) and annual evolution of cloudiness, precipitation, and aerosol concentration (Fig. 7) shows that from January to April, $<\bar{K}t>$ value increased from 45.5% to 59.0% as a result of the decrease in cloudiness from 60.7% to 33.0%; relative humidity from 77.5% to 74.2%, and precipitation from 246mm to 66mm in the same period. January, in which ZCAS is always more intense, had the lowest transmissivity of $\bar{H}_G$ irradiation in the year, $<\bar{K}t>$=45.5 %, while April had the highest transmissivity of $\bar{H}_G$ irradiation in the year, $<\bar{K}t>$=59.0%.

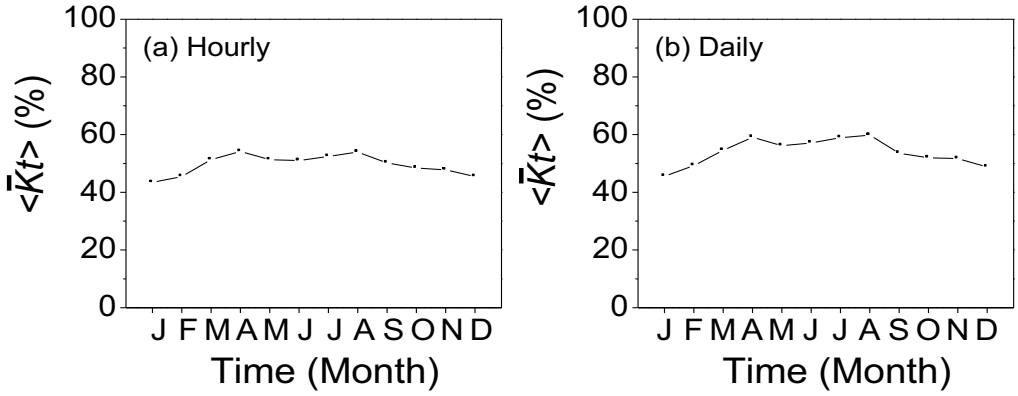

Fig. 9: Hourly and daily annual evolution of $<\bar{K}t>$ among years.

The result obtained in the month of April can be attributed to the transition between rainy and dry periods, in which a marked reduction in cloudiness and precipitation is observed compared to the previous months. After a reduction in frequency of occurrence and intensity in the southeastern region (region of Botucatu city), the CZSA moves gradually to the northern region of the country, allowing incoming cold fronts from the south polar region, which decrease temperature and lower concentration of clouds and water vapor in the atmosphere. The analysis of sky coverage in this period shows that in January, 30.0% of days were totally cloudy; 42.0% of days were partially diffuse (days in which direct irradiation is lower than diffuse irradiation); 22.0% of days were partially clear (days in which diffuse irradiation is lower than direct irradiation) and 8.0% of days were clear, while in April, 10.0% of days were totally cloudy; 18.0% of days were partially diffuse; 27,0% of days were partially clear, and 44.0% of days were clear. The decrease in $<\bar{K}t>$ value to 56.2% in May compared to the value of $<\bar{K}t>$=59.0% in April was a result of incoming polar cold fronts which increased cloudiness, precipitation and humidity. The percentage of cloudy sky days in May in relation to those in April increased from 10.0% to 14.0%, while the percentage of clear sky days decreased from 44.4% to 37.2%, respectively. From May to August, a dry period and with occurrences of burning of sugar cane, $<\bar{K}t>$ value increased from 56.2% to 59.8% as a result of the decrease in cloudiness from 0.35% to 0.27%, precipitation from 74.9% to 36.3% and relative humidity from 74.8% to 67.8%, and the increase in aerosol concentration in the atmosphere from 23.0µg/m^3 to 45.0µg/m3. In September, in which the sky coverage had the highest aerosol concentration, the decrease in $<\bar{K}t>$ value to 53.6% in relation to 59.8% in August was also a result of increased cloudiness, relative humidity and aerosol concentration. Considering all sky coverage, characterizing individual effects of aerosol, clouds and water vapor on the extinction of global radiation is not possible. Values of $<\bar{K}t>$ decreased from 52.0% to 48.7% in October,

November and December, as a function of increased cloudiness from 46.0% to 52.0%, precipitation from 108 mm to 203 mm and relative humidity from 70.0% to 75.0%. These increases were a result of humid frontal systems from the Atlantic Ocean and the beginning of ZCAS.

Fig. 10(a, b) shows annual evolution of hourly and daily $<\bar{K}_{bh}>$ and $<\bar{K}_{d}>$ fractions among years calculated by Eq. (7):

$$< \bar{\boldsymbol{K}}_{\boldsymbol{bh}} > = \sum_{j=1}^{m}(\bar{\boldsymbol{K}}_{\boldsymbol{bh}}/m); < \bar{\boldsymbol{K}}_{\boldsymbol{d}} > = \sum_{j=1}^{m}(\bar{\boldsymbol{K}}_{\boldsymbol{d}}/m) \qquad (7)$$

in which, $\bar{\boldsymbol{K}}_{\boldsymbol{bh}} = \sum_{\boldsymbol{i=1}}^{\boldsymbol{n}}(\boldsymbol{H_G}/\boldsymbol{H_{bh}})/\mathrm{n}$; $\bar{\boldsymbol{K}}_{\boldsymbol{d}} = \sum_{\boldsymbol{i=1}}^{\boldsymbol{n}}(\boldsymbol{H_G}/\boldsymbol{H_d})/\mathrm{n}$,

and n is the number of hours and days per year and j is the number of years.

Seasonal variation is a result of variations in cloudiness, water vapor and aerosol concentration among years in the local atmosphere. The annual evolution of $<\bar{K}_{bh}>$ and $<\bar{K}_{d}>$ fractions is inverse and symmetrical in time: value of $<\bar{K}_{bh}>$ is lower than that of $<\bar{K}_{d}>$ in the rainy period in January, February, October, November and December, in which values of cloudiness, precipitation and water vapor are the highest in the year. On the contrary, value of $<\bar{K}_{bh}>$ fraction is lower than that of $\bar{K}_{d}$ fraction in the dry period, April, May, June, July and August, in which cloudiness, precipitation and water vapor are lower and aerosol concentration is the highest in the year. The $<\bar{K}_{bh}>$ and $<\bar{K}_{d}>$ fractions are roughly the same in months of transition between humid and dry periods, March and September.

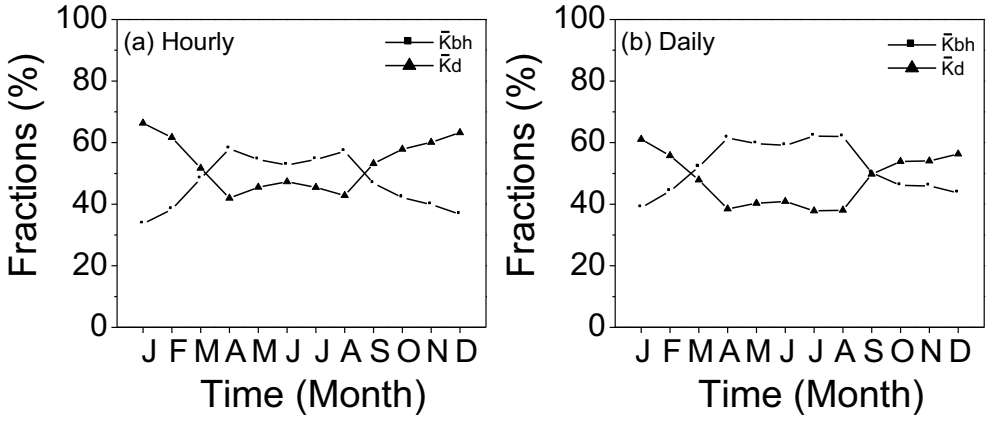

Fig. 10(a, b): Hourly and daily annual evolution of $<\bar{K}_{bh}>$ and $<\bar{K}_{d}>$ fractions among years.

The value of $<\bar{K}_{bh}>$ fraction increased from the least percentage of 33.6% (hourly) and 38.9% (daily) in the most humid and cloudy month (January) to the highest percentage of 58.0% (hourly) and 61,4% (daily) in the humid and cloudless month of April. On the contrary, in this period, the value of $<\bar{K}_{d}>$ fraction decreased from the highest value of 66.4% (hourly) and 61.1% (daily) in the most cloudy and humid month (January) to the lowest value of 42,0% (hourly) and 38.6% (daily) in the humid and cloudless month of April. Values of hourly and daily $<\bar{K}_{bh}>$ and $<\bar{K}_{d}>$ fractions from April to August show an inverse and symmetric inflexion point in June: while the value of $<\bar{K}_{bh}>$ fraction decreased from 58.0% (hourly) and 61.4% (daily) to 52.7% (hourly) and 59.4% (daily), from April to June, as a result of the increase in cloudiness, precipitation and water vapor in the atmosphere, the value of $<\bar{K}_{d}>$ fraction increased from 42.0% (hourly) and 38.6% (daily) to 47.3% (hourly) and 40.6 % (daily). From June to August, while $<\bar{K}_{bh}>$ fraction increased from 52.7 % (hourly) and 59.4% (daily) to 57.2% (hourly) and 61.9% (daily), due to the decrease in cloudiness, precipitation and water vapor in the atmosphere, the value of $<\bar{K}_{d}>$ fraction decreased from 47.3% (hourly) and 40.6% (daily) to 42.8% (hourly) and 38.1% (daily). In months of August until December, the value of $<\bar{K}_{bh}>$ fraction decreased from the highest percentage of 57.2% (hourly) and 61.9% (daily) in the clearest and driest month (August) to the lowest percentage of 36.8% (hourly) and 43.6% (daily) in the cloudy and humid month (December). Inversely, the value of $<\bar{K}_{d}>$ fraction increased

from 42.8% (hourly) and 38.1% (daily), in the clear and dry month of August to 63.2% (hourly) and 56.4% (daily) in the cloudy and humid month of December.

4. CONCLUSIONS

The objective of this study was to perform a statistical and climatic analysis of a data base of direct and diffuse global radiation measured from 1996 to 2006 in the city of Botucatu, SP, Brazil.

Results showed that hourly and daily annual mean $<\bar{H}_G>$, $<\bar{H}_{bh}>$ and $<\bar{H}_d>$ irradiation among years were as follows: $<\bar{H}_G>$=1.49MJ/m^2 and $<\bar{H}_G>$=17.74 MJ/m^2; $<\bar{H}_{bh}>$=0.90MJ/m^2 and $<\bar{H}_{bh}>$=10.33MJ/m^2 and $<\bar{H}_d>$=0.57MJ/m^2 and $<\bar{H}_d>$=7.09 MJ/m^2. Values of monthly mean $<\bar{H}_G>$, and $<\bar{H}_d>$ irradiation among years were higher in the south solar declination in January, February, March, October, November and December, in which the concentrations of clouds and water vapor in the atmosphere are the highest in the year. On the contrary, values of irradiation were lower in the north solar declination in April, May, June, July, August and September, in which the concentrations of clouds and water vapor are the lowest, and the concentration of aerosols is the highest in the year. Value of $<\bar{H}_{bh}>$ was higher in April, March, August and September, with alternating cloudy and humid months as March and September and clearer and drier months as April and August. Hourly $<\bar{H}_G>$ irradiation ranged from 1.65MJ/m^2 in March to 1.16MJ/m^2 in June; $<\bar{H}_{bh}>$ irradiation ranged from 1.06MJ/m^2 in April to 0.79MJ/m^2 in June, $<\bar{H}_d>$ irradiation ranged from 0.70MJ/m^2 in January to 0.37MJ/m^2 in June and July. Similarly, daily $\bar{H}_G$ irradiation ranged from 21.35MJ/m^2 in November to 12.94MJ/m^2 in June; $<\bar{H}_{bh}>$ irradiation ranged from 11.83MJ/m^2 in April to 8.49MJ/m^2 in June, and $<\bar{H}_d>$ irradiation ranged from 10.29MJ/m^2 in December to 4.38MJ/m^2 in June.

Annual evolution of hourly and daily $<\bar{K}t>$ clarity indexes among years shows that in rainy periods from January to April, $<\bar{K}t>$ value increased from 43.5% to 54.2% (hourly) and 45.6% to 59.1% (daily) as a result of decreased cloudiness, precipitation and water vapor in the atmosphere. Similarly, in October, November and December, values of $<\bar{K}t>$ decreased from 48.4% to 45.4% (hourly) and 52.0% to 48.8% (daily). In the dry period of May, the decrease in $<\bar{K}t>$ value to 51.3% (hourly) and 56.2% (daily) was a result of the increase in cloudiness, precipitation and water vapor in the atmosphere. From May to August, $<\bar{K}t>$ value increased to 53.9% (hourly) and 59.8% (daily) as a result of the decrease in cloudiness, precipitation and water vapor in the atmosphere, and of the increase in aerosol concentration in the atmosphere. In September, the decrease in $<\bar{K}t>$ value to 50.2% (hourly) and 53.6% (daily) was a result of increased cloudiness, water vapor in the atmosphere and aerosol concentration.

The value of $<\bar{K}_{bh}>$ fraction increased from the least percentage of 33.6% (hourly) and 38.9% (daily) in the most humid and cloudy month (January) to the highest percentage of 58.0% (hourly) and 61.4% (daily) in the humid and cloudless month of April. In this period, the value of $<\bar{K}_d>$ fraction decreased from the highest value of 66.4% (hourly) and 61.1% (daily) to the lowest value of 42.0% (hourly) and 38.6% (daily). From April to June, value of $<\bar{K}_{bh}>$ fraction decreased from 58.0% (hourly) and 61.4% (daily) to 52.7% (hourly) and 59.4% (daily) as a result of increased cloudiness, precipitation and water vapor in the atmosphere, while the value of $<\bar{K}_d>$ fraction increased from 42.0% (hourly) and 38.6% (daily) to 47.3% (hourly) and 40.6% (daily). From June to August, while $<\bar{K}_{bh}>$ fraction increased from 52.7% (hourly) and 59.4% (daily) to 57.2% (hourly) and 61.9% (daily), due to the decrease in cloudiness, precipitation and water vapor in the atmosphere, the value of $<\bar{K}_d>$ fraction decreased from 47.3% (hourly) and 40.6% (daily) to 42.8% (hourly) and 38.1% (daily). In months of August to December, the value of $<\bar{K}_{bh}>$ fraction decreased from the highest percentage of 57.2% (hourly) and 61.9% (daily) in the clearest and driest month (August) to the lowest percentage of 36.8% (hourly) and 43.6% (daily) in the cloudy and humid month (December). In this period, the value of $<\bar{K}_d>$ fraction increased from 42.8% (hourly) and 38.1% (daily), to 63.2% (hourly) and 56.4% (daily).

REFERENCES

Carvalho, L. M. V.; Jones, C.; Liebmann, B.. Extreme precipitation events in sputheastern South America and large-scale convective patters in the South Atlantic Convergence Zone. Jornal of Climate, v. 15, p. 2377-2394, 2002.

Cavalcanti, E.S.C., 1991. Analysis of experimental solar radiation for Rio de Janeiro, Brazil. *Solar Energy*, v.47, p.231-235.

Codato, Georgia, Oliveira, A. P., Soares, Jacyra, Escobedo, J. F., Gomes, E.N., Dal Pai, A., 2007. Global and diffuse solar irradiances in urban and rural areas in southeast of brazIL. Theoretical and Applied Climatology. v.1, p.12.

De Miguel, A., Bilbao, J., Aguiar, R., Kambezidis, H., Negro, E. Diffuse solar irradiation model evaluation in north Mediterranean belt area. Solar Energy, v.70, n.2, p.143-53, 2001.

Erbs, D.G., Klein, S.A., Duffie, J.A. Estimation of the diffuse radiation fraction for hourly, daily and monthly-average global radiation. Solar Energy, v.28, p.293-302, 1982.

Hawlader, M. N. A. Diffuse, global and extraterrestrial solar radiation for Singapore. International Journal of Ambient Energy, v.5, p.31-8, 1984.

Jacovides, C. P., Hadjioannou, L., Pashiardis, S., Stefanou, L. On the diffuse fraction of daily and monthly global radiation for the island of Cyprus. Solar Energy, v.56, n.6, p.565-72, 1996.

Lalas, D. P., Petrakis, M., Papadopoulos, C. Correlations for the estimation of the diffuse radiation component in Greece. Solar Energy, v.39, n.5, p.455-8, 1987.

Lam, J.C., Li, D.H.W. Correlations between global solar radiation and its direct and diffuse components. *Build. and Environ.*, v.31, p.527-35, 1996.

Liu, B. Y. H., Jordan, R. C. The interrelationship and characteristic distribution of direct, diffuse and total solar radiation. Solar Energy, v.3, n.4, p.1-19, 1960.

Newland, F. J. A study of solar radiation models for the coastal region of south China. Solar Energy, v.43, n.4, p.227-35, 1989.

Nogués-Paegle, J.; MO, K.C. Alternating wet and dry conditions over South America during summer. Mon Wea Rev, v. 125, p 279-291, 1997.

Lemos, C.F.; Calbete, N. O. Sistemas frontais que atuaram no litoral de 1987-1995. *Climanálise*, Edição comemorativa 10 anos, 1996. (INPE-10717-PRE/6178).

Liebmann, B.; Jones, C.; Carvalho, L. M. V. Interannual variability of daily extreme precipitation events in the state of São Paulo, Brazil. *J. Climate*, 14, p. 208–218, 2001.

Louche, A., Notton, G., Poggi, P., Simonnot, G. Correlations for direct normal and global horizontal irradiation on a French Mediterranean site. *Sol. Energy,* v.46, p.261-66, 1991.

Oliveira, A.P., Escobedo, J.F., Machado, A.J., Soares, J., 2002. Correlation models of diffuse-solar radiation applied to the city of São Paulo, Brazil. Applied Energy, v.71, p.59-73.

Oliveira, A.P., Machado, A.J., Escobedo, J.F., Soares, J., 2002. Diurnal evolution of solar radiation at the surface in the city of São Paulo: seasonal variation and modeling. Theor. Appl. Clim., v.71, p.231-250.

Reindl, D. T., Beckman, W. A., Duffie, J. A. Diffuse fraction correlations.Solar Energy, v.45, n.1, p.1-7, 1990.

Satyamurty, P.; Nobre, C. A.; Silva Dias, P. L. Topics: South America. **Meteorological Monographs**, v.27, n.49, p.119-139, 1998.

Satyamurti,P e L.F.Mattos, 1989. Climatologycal lower trophosferic frontogenesis in the midlalatitudes due to horizontal deformation and divergence.Mon.Wea. Rev.,108:410-520.

Soares, J., Oliveira, A.P., Boznar, M.Z., Mlakar, P., Escobedo, J.F., Machado, A.J., 2004. Modeling hourly diffuse solar-radiation in the city of São Paulo using a neural-network technique. Applied Energy, v.79, p.201-204.

Souza, J.L., Nicácio, R.M., Moura, M.A.L., 2005. Global solar radiation measurements in Maceió, Brazil. Renewable Energy, v.30, p.1203-1220.

Tiba, C. Aguiar, R., Fraidenraich., 2005. N. Analysis of a new relationship between monthly global irradiation and sunshine hours from a database of Brazil. Renewable Energy, v.30, p.957-966.